



Molecular Entomology

Trehalose promotes the response of CYP genes in *Tribolium castaneum* (Coleoptera: Tenebrionidae) to high-CO₂ stress

Yuhang Xie[®], Min Zhou, Liwen Guan, Sijing Wan, Yi Zhang, Xinyi Zhang, Yuya Zhang, Xinyu Zhang, Yan Li, and Bin Tang* [®]

College of Life and Environmental Sciences, Hangzhou Normal University, Hangzhou, P.R. China

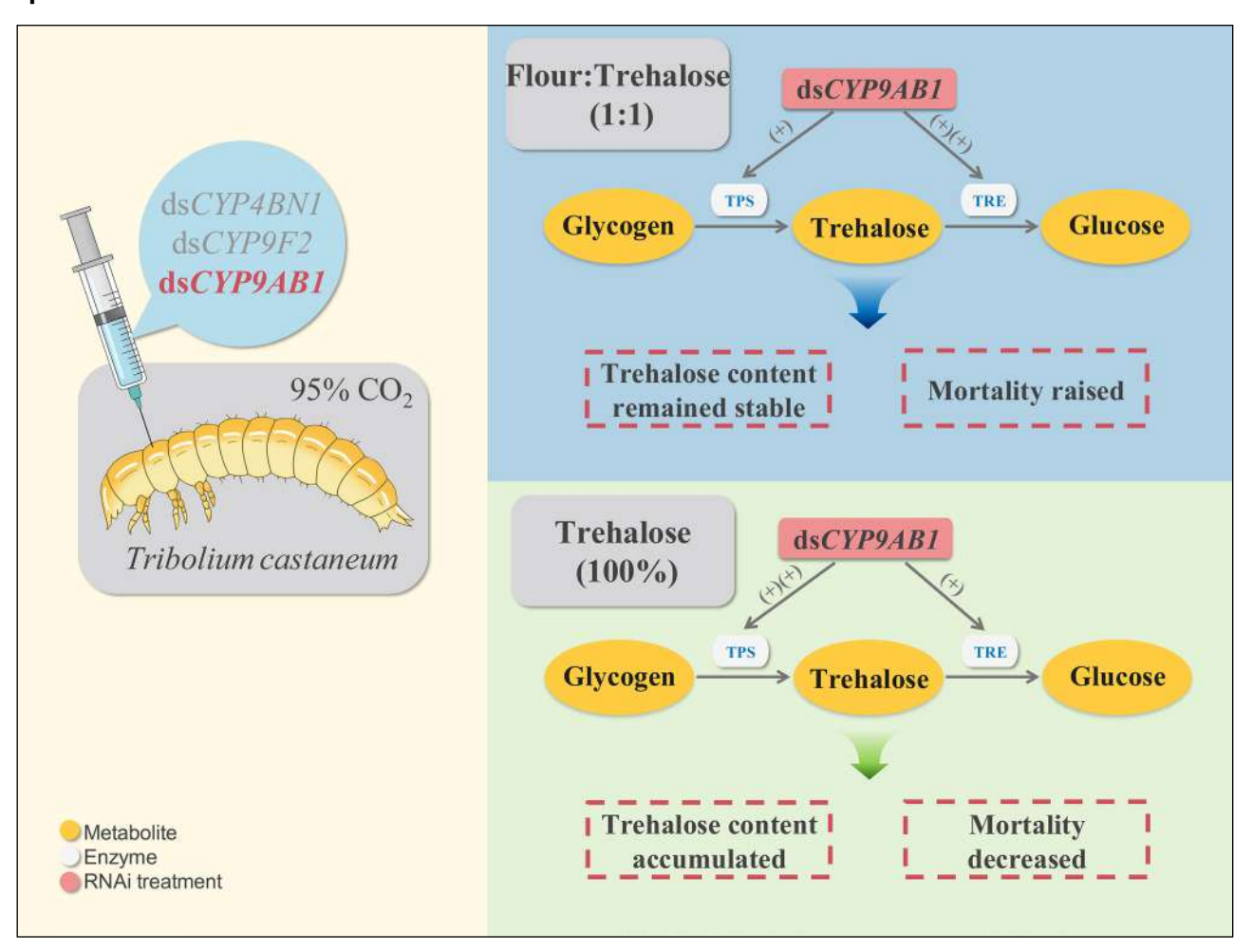
*Corresponding author. College of Life and Environmental Sciences, Hangzhou Normal University, Hangzhou, Zhejiang 311121, P.R. China (Email: tbzm611@hznu.edu.cn).

Subject Editor: Michael Brewer

Cytochrome P450 monooxygenases (CYP450) and trehalose play a significant detoxification role under high CO₂ stress. Notably, CYP450 significantly affects trehalose metabolism of *Tribolium castaneum* (Herbst) (Coleoptera: Tenebrionidae), a devastating stored pest. To explore whether trehalose enhances CYP gene responses to CO₂ stress, investigations were conducted on the 95% CO₂ tolerance in 8th-instar *T. castaneum* larvae, whose specific CYP genes–*TcCYP4BN1*, *TcCYP9F2*, and *TcCYP9AB1*—were silenced, across different trehalose dietary regimes (50% flour + 50% trehalose or 100% trehalose). The 95% CO₂ tolerance response was systematically evaluated through multi-dimensional analysis of gene expression levels, carbohydrate contents, and enzyme activities. Results indicated that compared with the 50% flour + 50% trehalose feeding regimen, trehalose-only diet groups exhibited downregulation of trehalose metabolism-related genes, with the notable exception of the ds*CYP9F2* experimental group. As to carbohydrate contents, glucose content increased significantly on 100% trehalose diet by inhibiting the expression of *TcCYP9AB1*, but it decreased in the other 2 groups, a pattern that also held true for glycogen. Together, these results demonstrate that trehalose does enhance the response of CYP genes to CO₂ stress, and that *TcCYP9AB1* is more responsible for modulating trehalose metabolism. Future research could investigate the molecular mechanisms underlying these regulatory processes and their practical applications, potentially enhancing biocontrol techniques and advancing pest management solutions.

Keywords: trehalose, cytochrome P450 monooxygenase, CO₂ stress, stored pest, RNA interference

Graphical abstract



Introduction

Food grain is an important material basis for human survival and an important strategic material for the national economy and livelihood of some (Cui et al. 2023). However, during the food storage stage, the activity of pests has given rise to great losses on grain storage (Ingegno and Tavella 2022). Among these destructive insects, Tribolium castaneum (Herbst) (Coleoptera: Tenebrionidae), a prevalent stored pest, causes substantial economic losses in diverse storage environments (Manandhar et al. 2018, Natonek-Wiśniewska et al. 2022). To control these pests, modified atmosphere storage technology, utilizing carbon dioxide or nitrogen to alter the gas composition, is gaining popularity as a safe and cost-effective solution relative to chemical fumigants (Paul et al. 2020). High N₂ is believed to reduce O, levels (Huang et al. 2024a), while CO, (10 to 20%) can be directly toxic or inhibitory to insects (Badre et al. 2005). In Rhyzopertha dominica (Fabricius) (Coleoptera: Bostrichidae), higher mortality rates have been observed with the rising CO, gas pressure (Sadeghi et al. 2021). Also, in Plodia interpunctella (Hübner) (Lepidoptera: Pyralidae), more significant decrease in survival rates has been noted after CO, was added to low O₂ (Huang et al. 2024b). Despite remarkable strides in modified atmosphere storage technology, the development of resistance to high CO, levels in pests has presented

considerable challenges to widespread adoption and practical application (Wu et al. 2022). Therefore, investigating the molecular mechanisms behind CO₂-enriched modified storage technology could further influence and improve the field of grain preservation.

Trehalose is known for its role as a biochemical protector in promoting organismal survival under adverse environmental stress (Watanabe 2006, Ribeiro et al. 2024). As a non-reducing disaccharide widely distributed in nature, trehalose can be synthesized by trehalose-6-phosphate synthase (TPS) and degraded by trehalase (TRE) (Kaur et al. 2024). TPS is broadly categorized into 2 subfamilies: class I and class II (Wang et al. 2019, Zou et al. 2024), while TRE is categorized into 2 forms based on its cellular distribution: the soluble form, Trehalase 1 (TRE1), and the membrane-bound form, Trehalase 2 (TRE2) (Tellis et al. 2023, Zhang et al. 2024). As early as 2003, trehalose has been reported to enhance hypoxia adaptability mainly by reducing protein aggregation in cells (Chen et al. 2003), and it has currently found to help insects cope with various abiotic and biotic stresses (Tao et al. 2023). Due to these properties, its protective effects under toxic stress are of great interest (Singh et al. 2011, Bao et al. 2021), and its metabolic pathways are being considered as targets for pest control (Tang et al. 2016, Pan et al. 2020, Wu et al. 2022).

In addition to trehalose-mediated protection, the cytochrome P450 monooxygenase (CYP450) gene families, among the largest in nature, also contribute to environmental stress tolerance across animals, plants, and microorganisms (Baldwin et al. 2021, Shelomi 2022, Chakraborty et al. 2023). In Apis cerana cerana (Fabricius) (Hymenoptera: Apidae) and T. castaneum, specific CYP genes are reportedly involved in pesticide resistance and detoxification (Zhang et al. 2021, Tan et al. 2023). Furthermore, CYP genes are also responsively expressed and participate in resistance mechanisms under physical stressors such as hypoxia and ultraviolet radiation (Sang et al. 2012, Zhu et al. 2016). These findings suggest that understanding the underlying mechanisms is crucial for discovery of novel control targets and strategies, with some reports highlighting the importance of CYP450 in T. castaneum's response to extreme environments (Yao et al. 2019, Wang et al. 2020, Chen et al. 2022). However, the same function in insects lacks enough research (Pender and Horvitz 2018), signaling a need for more scientific investigations.

In the current study, experiments were conducted on the 95% CO₂ tolerance of 8th-instar *T. castaneum* larvae where we silenced *TcCYP4BN1* (GenBank: NM_001130521 (National Center for Biotechnology Information 2024a), NCBI Nucleotide Database), *TcCYP9F2* (GenBank: NM_001134234 (National Center for Biotechnology Information 2024b), NCBI Nucleotide Database), and *TcCYP9AB1* (GenBank: XM_967453 (National Center for Biotechnology Information 2024c), NCBI Nucleotide Database) genes, which may be correlated with the trehalose metabolism pathway, across different trehalose regimes (50% flour + 50% trehalose or 100% trehalose). We sought to investigate whether trehalose enhances the response of CYP genes to CO₂ atmosphere stress, offering new solutions to the problem of pest resistance in grain storage under controlled atmosphere conditions.

Materials and Methods

Insect Cultures

The insects *T. castaneum* were sustained under laboratory conditions with the whole wheat flour as the primary nutrient source. The rearing environment was precisely controlled, with

temperature regulated at 29 ± 1 °C, humidity maintained at 65 ± 5 % RH, and a 0L : 24 D photoperiod implemented throughout the cultivation period.

RNA Extraction and cDNA Synthesis

Total RNA extraction from *T. castaneum* larval specimens was conducted using the Trizol reagent kit (Invitrogen, Carlsbad, California, United States). The extracted RNA quality verification involved dual assessment procedures: 1µl RNA for purity/concentration determination using the NanoDrop 2000 spectrophotometer (Thermo Fisher Scientific, Waltham, Massachusetts, United States), and 2 µl RNA for structural integrity confirmation via 1% agarose gel electrophoresis (Kim et al. 2024). Any residual RNA was maintained at –80 °C for future analysis. The first-strand cDNA synthesis was achieved using the PrimeScript RT Reagent Kit With gDNA Eraser (TaKaRa, Kyoto, Japan) and stored at –20 °C (Tang et al. 2016).

Cloning of *TcCYP4BN1*, *TcCYP9F2*, and *TcCYP9AB1* Genes

Partial ORF sequences of TcCYP4BN1, TcCYP9F2, and TcCY-P9AB1 were amplified from the synthesized cDNA using the Ex Tag kit (TaKaRa, Kyoto, Japan) (Osanai et al. 2006). Specific primers for amplification (Table 1) were designed with Primer 6.0 software (Premier Biosoft International, Palo Alto, California, United States) (Long et al. 2024). After confirming these amplified target fragments by electrophoresis, the corresponding gel bands were excised and purified with the DNA Gel Extraction Kit (US Everbright, Jiangsu, China). Quality and concentration of the purified DNA were assessed using a NanoDrop 2000 spectrophotometer prior to -20 °C storage (Kim et al. 2024). To obtain the connecting solution, 3 µl of the purified DNA were mixed with 3.5 ul Solution I and 0.5 ul pMD18-T Vector Cloning Kit (Takara, Kyoto, Japan) in PCR tubes, followed by brief centrifugation and incubation at 16°C for 30min (Zhang et al. 2020). Plasmid transformation was performed using DH5α competent cells, after which distinct circular colonies from the Petri dish were selected, dissolved in 30 µl of sterile water, and directly utilized as templates for colony PCR to verify cloning

Table 1. Primer sequences used for dsRNA synthesis and qRT-PCR detection of genes associated with trehalose metabolism in T. castaneum

Gene	Forward Primer (5'-3')	Reverse Primer (5'-3')	Function of Primers
dsCYP4BN1	GCATCAACGAGAAGTCCACA	AGTCAGCAAACCAGTCCCTAA	dsRNA synthesis
dsCYP4BN1-T7	T7-GCATCAACGAGAAGTCCACA	T7-AGTCAGCAAACCAGTCCCTAA	
dsCYP9AB1	GTTCTATCTGATGAGCAAAGC	CGATGACGTACTCCTTCG	
dsCYP9AB1-T7	T7-GTTCTATCTGATGAGCAAAGC	T7-CGATGACGTACTCCTTCG	
dsCYP9F2	CCTACAAATACTGGACCGA	CAGGAAGTACCCCAACAA	
dsCYP9F2- T7	T7-CCTACAAATACTGGACCGA	T7-CAGGAAGTACCCCAACAA	
TcCYP4BN1	GGCAGGCCTCTAACTCAAGA	CGTAACTGCGGGACTTTTGT	qRT-PCR detection
TcCYP9AB1	GGGCGTCACGATACCAGATA	TCCTCCCAGATGAAGTGCTG	
TcCYP9F2	ACCGGCTACCAAGAATCCAA	GTGACCTTTCCGTTGCAGTT	
TcTRE1-1	AACGACTCGCAATGGCTGG	CGGAGGCGTAGTGGAATAGAG	
TcTRE1-2	GTGCCCAATGGGTTTATCG	CAACCACAACACTTCCTTCG	
TcTRE1-3	CCTCTCATTCGTCACAAGCG	AAGCGTTTGATTTCTTTGCG	
TcTRE1-4	ACGGTGCCCGCATCTACTA	GTGTAGGTGGTCCCGTTCTTG	
TcTRE2	CTCAGCCTGGCCCTTAGTTG	GGAGTCCTCGTAGATGCGTT	
TcTPS1	CGATTCGTACTACAACGGCTGC	GTGGTGTAGCATTGCCAGTGC	
TcTPS2	ACCTTGCCATCATCCCTCC	GCCCACCATTTGCTTCACA	
TcRPL13a	ACCATATGACCGCAGGAAAC	GGTGAATGGAGCCACTTGTT	

success. After PCR amplification, 1% agarose gel electrophoresis was used to detect the correctness of the target fragment of the colony amplified using PCR. Positive clones were cultured overnight in LB-Amp medium (37°C, 250 rpm). Then, 500 µl of the clones were submitted to Zhejiang Sunya Biotech Co., Ltd (Zhejiang, China) for sequencing. Following the same method, the Green fluorescent protein gene (GFP) was cloned by using the pMD18-T plasmid with the GFP sequence as the template.

Synthesis and Microinjection of dsRNA

The primers (Table 1) designed using Primer 6.0 software with a T7 promoter were used to perform cross-PCR reaction on the correctly sequenced plasmids, after which the double-stranded RNA (dsRNA) of the target genes were synthesized via the T7 RiboMax Express RNAi System kit (Promega, Madison, Wisconsin, United States) (Xu et al. 2020, Long et al. 2024). The total RNA integrity and concentration were verified through agarose gel electrophoresis and spectrophotometry separately. The ds*GFP* was synthesized for the control group using the same method. Synthesized products were finally stored at -80 °C.

Tribolium castaneum larvae at the eighth instar were immobilized on ice and microinjected using a Transferman 4r microinjection (Eppendorf, Hamburg, Germany) with 100 nL dsRNA (2,000 ng/µl) targeting TcCYP4BN1, TcCYP9F2, or TcCYP9AB1 through the abdominal intersegmental membrane (second-third segments) (Guan et al. 2024). The same amount of dsGFP was injected into the control group. Each dsRNA injection group had about 800 larvae in total.

Experimental Setup

Following microinjection with dsCYP4BN1, dsCYP9F2, dsCYP9AB1, or dsGFP, larvae from each injection group were randomly divided into 2 equal subgroups (about 400 larvae per subgroup). These subgroups were then fed 2 distinct trehalose dietary regimens: 1 subgroup received 50% flour + 50% trehalose, and the other received 100% trehalose. This experimental setup created a total of 8 final treatment groups (4 dsRNA types × 2 diets). After 48 h, we evaluated mortality rates from each treatment group. Surviving larvae (minimum 260 per group) were collected and stored at $-80\,^{\circ}\text{C}$ for a subsequent analysis of gene expression levels, carbohydrate contents, and enzyme activities.

Mortality Analysis

Larvae that died within 3 h of microinjection were identified as mechanical injury death and excluded from subsequent mortality analysis. Mortality rates were evaluated after 48 h of microinjection in each group maintained under 95% $\rm CO_2$ with either 50% flour + 50% trehalose or 100% trehalose diets. For each treatment group, a minimum of 370 larvae were used for mortality calculation, with 4 biological replicates per treatment group. Larvae were recorded death if they were immobile after being touched with a brush.

Quantitative Real-Time Polymerase Chain Reaction

Tribolium castaneum larvae that survived in the 48-h mortality assessment were collected from the 8 previously described treatment groups. Each treatment group combined 1 of 4 dsRNA microinjections (dsCYP4BN1, dsCYP9F2, dsCYP9AB1, or dsGFP) with 1 of 2 trehalose dietary regimens (50% flour +

50% trehalose or 100% trehalose) under a 95% CO, atmosphere. Three biological replicates (10 larvae each) were analyzed per group. For each biological replicate, 3 technical replicates were performed to ensure experimental reliability. Utilizing Primer 6.0 software, quantitative real-time polymerase chain reaction (qRT-PCR) primers (Table 1) were designed based on coding sequences of trehalose pathway genes in T. castaneum, with Ribosomal Protein L13a (RPL13a) serving as endogenous reference (Long et al. 2024). Gene expression quantification employed TB Green Premix Ex Tag II (Tli RNaseH Plus) (TaKaRa, Kyoto, Japan) on a Bio-Rad CFX96 system. qRT-PCR reaction system: 5 µl of an SYBR Green master mix, 0.4 µl (10 pmol) of forward/reverse primers, 1 µl of cDNA, 2.8 µl of RNase Free ddH₂O. qRT-PCR reaction procedure: pre-denaturation at 95 °C for 30 s, denaturation at 95 °C for 5 s, extension at 60 °C for 20 s (39 cycles). The melt curve analysis was conducted in a range of 65 to 95 °C. Relative expression was analyzed using 2-\triangletic CT methodology (Livak and Schmittgen 2001).

Determination of Carbohydrate Contents and Trehalase Activity

Samples for determining carbohydrate contents and trehalase activity were collected from the larvae that survived in the 48-h mortality assessment in the 8 previously described treatment groups. Each treatment group combined 1 of 4 dsRNA microinjections (dsCYP4BN1, dsCYP9F2, dsCYP9AB1, or dsGFP) with 1 of 2 trehalose dietary regimens (50% flour + 50% trehalose or 100% trehalose) under a 95% CO, atmosphere. Four biological replicates (15 larvae each) were analyzed per group. Following homogenization in 1,000 µl PBS (pH 7.0), samples underwent 30-min sonication and primary centrifugation (1,000×g, 20 min, 4°C). The resultant supernatant was divided into 2 aliquots: 350 µl for simultaneous quantification of glycogen, trehalose, and total protein, while the remaining 350 µl was ultracentrifuged (20,800×g, 60 min). After ultracentrifugation, 300 µl of ultra-supernatant and resuspended pellet (300 µl PBS) were respectively analyzed for glucose concentration, trehalase activity, and protein content. Trehalase activity assays incorporated 60 µl sample (supernatant/pellet suspension), 75 µl 40 mM trehalose (Sigma-Aldrich, Saint Louis, Missouri, United States), and 165 ul PBS, incubated at 37 °C for 60 min prior to heat inactivation (100°C, 5 min). Reaction termination with 260 μl 12 N H₂SO₄ preceded trehalase activity measurement via Glucose (Go) Assay Kit (Sigma-Aldrich, Saint Louis, Missouri, United States) with absorbance value measured at 540 nm using a microplate reader (Thermo Fisher Scientific, Waltham, Massachusetts, United States). Protein determinations utilized the BCA Protein Assay Kit (Beyotime, Shanghai, China), while trehalose measurements followed anthrone methodologies (Zhang et al. 2017, Yu et al. 2020, Ge et al. 2021).

Determination of CYP450 Activity

Cytochrome P450 monooxygenase activity was determined using the Insect Cytochrome P450 Enzyme-Linked Immunosorbent Assay (ELISA) Kit (COIBO BIO, Shanghai, China). Samples for determining CYP450 activity were collected from the larvae that survived in the 48-h mortality assessment in the 8 previously described treatment groups. Each treatment group combined 1 of 4 dsRNA microinjections (dsCYP4BN1, dsCYP9F2, dsCYP9AB1, or dsGFP) with 1 of 2 trehalose

dietary regimens (50% flour + 50% trehalose or 100% trehalose) under a 95% $\rm CO_2$ atmosphere. For each group, 4 biological replicates (30 larvae each) were homogenized in 30 μ l PBS and flash-frozen. Prior to analysis, samples were thawed (2 to 8 °C), mixed with 270 μ l PBS, and centrifuged (2,500 rpm, 20 min) to collect the supernatant. Standard solutions (50 μ l per well) and diluted test samples (40 μ l diluent + 10 μ l sample) were loaded onto the ELISA plate. After adding 100 μ l enzyme conjugate (excluding blank wells), the plate was incubated at 37 °C for 60 min. Wells were washed 5 times with 20× diluted buffer (30s interval per wash), followed by sequential addition of 50 μ l substrates A and B for 15 min of dark incubation at 37 °C. Reactions were terminated with 50 μ l stop solution (blue-to-yellow color transition), and absorbance was measured at 450 nm within 15 min using a microplate reader.

Statistical Analysis

All data were organized with Microsoft Excel (Microsoft Corporation, Redmond, Washington, United States) and analyzed with IBM SPSS Statistics 23.0 (IBM Corporation, Armonk, New York, United States). Results are presented as mean ± standard error (SE) and visualized in bar graphs with GraphPad Prism 9.0.0 (GraphPad Software, Boston, Massachusetts, United States). For gene expression data, student's independent samples t-test was used to compare differences between the dsCYP treatment group and the dsGFP control group in RNA interference efficiency and expression levels of trehalose metabolic pathway genes (ie TRE1-1, TRE1-2, TRE1-3, TRE1-4, TRE2, TPS1, and TPS2). For data of mortality, carbohydrate contents (ie glucose, trehalose, and glycogen), and enzyme activities (ie soluble trehalase, membrane-bound trehalase, and CYP450), Shapiro-Wilk test and Levene's test were used first to test normality and homoscedasticity respectively. Where data (ie mortality on 100% trehalose diet, carbohydrate contents, and enzyme activities) were normal and homoscedastic, one-way analysis of variance (ANOVA) was then used to determine the effect of CYP genes knockdown. When the one-way ANOVA results were significant (P < 0.05), means were separated by Tukey Honestly Significant Difference (HSD) post-hoc test at $\alpha = 0.05$. However, since mortality data on 50% flour + 50% trehalose diet were non-normal and heteroscedastic, Welch's ANOVA was used to test if mortality differed between groups: dsGFP, dsCYP4BN1, dsCYP9F2, and dsCYP9AB1 (Delacre et al. 2018). When the mortality differences were significant (P < 0.05), Games-Howell post-hoc test at $\alpha = 0.05$ was used to examine pairwise differences between means (Zhang et al. 2022, Agbangba et al. 2024). As to gene expression analvsis (qRT-PCR), 3 biological replicates per treatment group were used, while 4 biological replicates per treatment group were applied for measurements of mortality rates, carbohydrate contents, and enzyme activities.

Results

Detection of Silencing Efficiency and Mortality after Feeding Trehalose under 95% CO₂

Tribolium castaneum larvae received dsCYP injections and were fed with diets of either 50% flour + 50% trehalose or 100% trehalose, to explore the effects of CYP450 and trehalose on their resistance to 95% CO_2 stress. Changes in expression of target genes were then monitored. The results indicated that trehalose

feeding still maintains the potency of RNA interference under 95% CO₂. Specifically, the expression of TcCYP4BN1, same as that of TcCYP9AB1, significantly decreased when trehalose was added (TcCYP4BN1: $t_{50\% \text{ flour} + 50\% \text{ trehalose}} = 8.249$, df = 4, P = 0.001; $t_{\text{trehalose}} = 6.334$, df = 4, P = 0.003; TcCYP9AB1: $t_{50\% \text{ flour} + 50\% \text{ trehalose}} = 6.978$, df = 4, P = 0.002; $t_{\text{trehalose}} = 4.123$, df = 4, P = 0.015; Fig. 1A and C). Also, expression levels of TcCYP9F2 notably fell far below those in the control groups ($t_{50\% \text{ flour} + 50\% \text{ trehalose}} = 9.061$, df = 4, P < 0.001; $t_{\text{trehalose}} = 25.148$, df = 4, P < 0.001; Fig. 1B).

After 48 h, mortality of *T. castaneum* was observed and analyzed. Results indicated that under a 95% CO₂ atmosphere, mortality rates fluctuated depending on RNAi and trehalose diet. On a mixed diet of 50% flour + 50% trehalose, the mortality increased in all dsCYP treatment groups (F=21.280, df=3, 6.078, P=0.001). On 100% trehalose diet, dsCYP4BN1 and dsCYP9F2 slightly increased the mortality, while dsCYP9AB1 decreased mortality compared with the control (F=8.272, df=3, 12, P=0.003; Fig. 2).

Effect on Carbohydrate Contents under 95% CO₂ after Trehalose Feeding and dsRNA

Under 95% CO, conditions, carbohydrate contents were assessed in *T. castaneum* subjected to a combination of trehalose dietary regimes (50% flour + 50% trehalose or 100% trehalose) and dsCYP treatments after 48 h. The results indicated that carbohydrate contents changed little (Fig. 3). As to glucose content, it was generally reduced in the dsCYP groups on 50% flour + 50% trehalose diet (F=3.922, df=3, 12, P=0.037), and significantly increased in the dsCYP9AB1 group on 100% trehalose diet (F=14.285, df=3, 12, P<0.001; Fig. 3A). Glycogen content increased in the dsCYP9AB1 group but decreased in the other 2 groups on 50% flour + 50% trehalose diet (F=5.070, df=3, 12, P=0.017). On 100% trehalose diet, compared with the dsGFP, both the dsCYP4BN1 and dsCYP9F2 treatment groups exhibited reduced glycogen content, while the dsCYP9AB1 demonstrated an increased glycogen content (F=2.798, df=3, 12, P = 0.085; Fig. 3C). Trehalose content showed no significant differences among groups on a mixed diet (F=0.490, df=3, 12, P = 0.696). However, on 100% trehalose diet, dsCYP groups had notably higher trehalose levels than the control (F = 5.016, df = 3, 12, P = 0.018). Overall, the trehalose content from 50% flour + 50% trehalose diet was slightly higher than that from 100% trehalose diet in T. castaneum (Fig. 3B).

Effect on Trehalase Activity under 95% CO₂ after Trehalose Feeding and dsRNA

After 48 h of co-treatments with trehalose dietary regimes (50% flour + 50% trehalose or 100% trehalose) and dsCYP under 95% CO₂, the trehalase activity was quantified. Soluble trehalase activity slightly decreased in both the dsCYP4BN1 and dsCYP9AB1 treatment groups on 50% flour + 50% trehalose diet, or diverged on 100% trehalose diet compared with the controls, while dsCYP9F2 maintained equivalent activity on 50% flour + 50% trehalose diet but increased on 100% trehalose diet, though no significant changes were observed in either diet condition ($F_{50\% \text{ flour} + 50\% \text{ trehalose}} = 0.968$, df = 3, 12, P = 0.440; $F_{\text{trehalose}} = 2.406$, df = 3, 12, P = 0.118; Fig. 4A). Membrane-bound trehalase activity remained stable on 50% flour + 50% trehalose diet (F = 1.495, df = 3, 12, P = 0.266) but dropped significantly by 22.4% with the dsCYP9AB1 treatment on 100% trehalose diet (F = 3.556, df = 3, 12, P = 0.048; Fig. 4B).

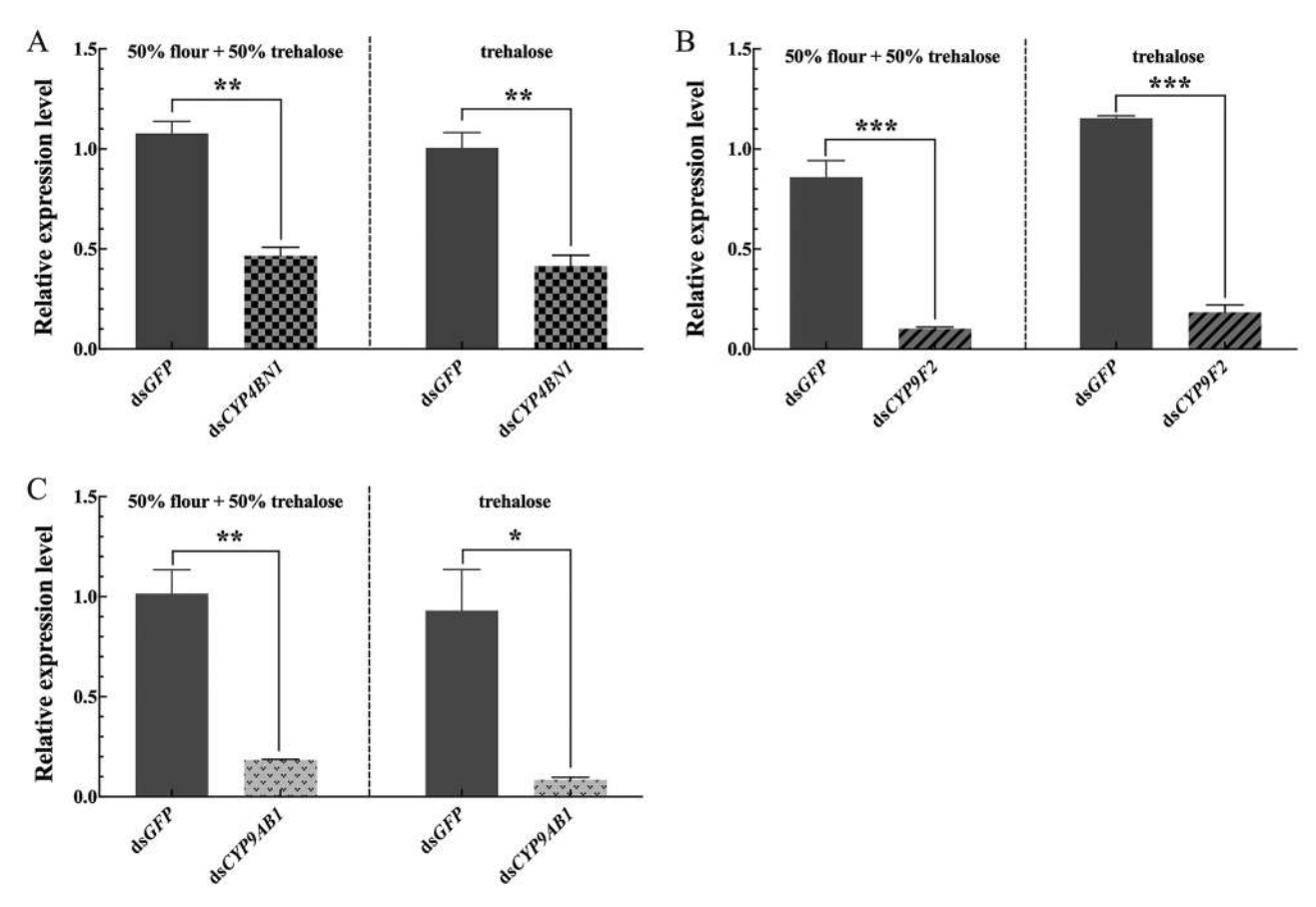


Fig. 1. The dsRNA interference efficiency in T. C C02 stress after 48 h of trehalose dietary regimes (50% flour + 50% trehalose or 100% trehalose) and ds C100% trehalose) and ds C110% trehalose) and ds C110% trehalose or 100% trehalose) and ds C110% trehalose) and ds C110% trehalose or 100% trehalose) and ds C110% trehalose) and ds C110%

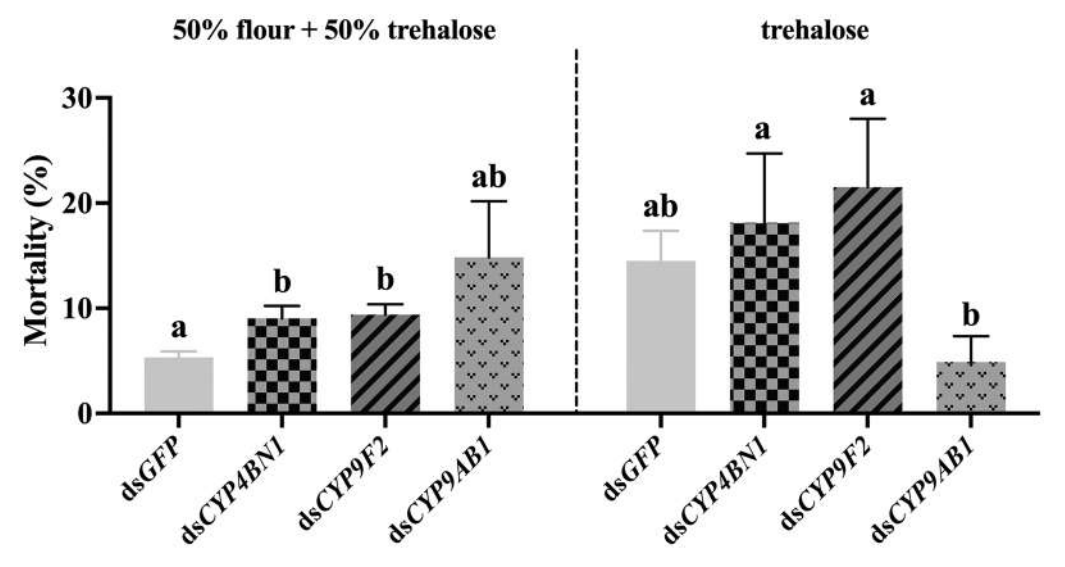


Fig. 2. Mortality in *T. castaneum* under 95% CO₂ stress after 48h of trehalose dietary regimes (50% flour + 50% trehalose or 100% trehalose) and ds *CYP* treatments (ds *GFP*, ds *CYP4BN1*, ds *CYP9F2*, or ds *CYP9AB1*). Each group included 4 biological replicates. Values are presented as mean \pm SE. Different letters indicate significant differences between groups. The 50% flour + 50% trehalose dietary groups were analyzed using Welch's ANOVA followed by Games-Howell post-hoc test at α = 0.05 (letters ordered from smallest to largest mean), while the 100% trehalose dietary groups were compared by one-way ANOVA followed by Tukey HSD post-hoc test at α = 0.05 (letters ordered from largest to smallest mean).

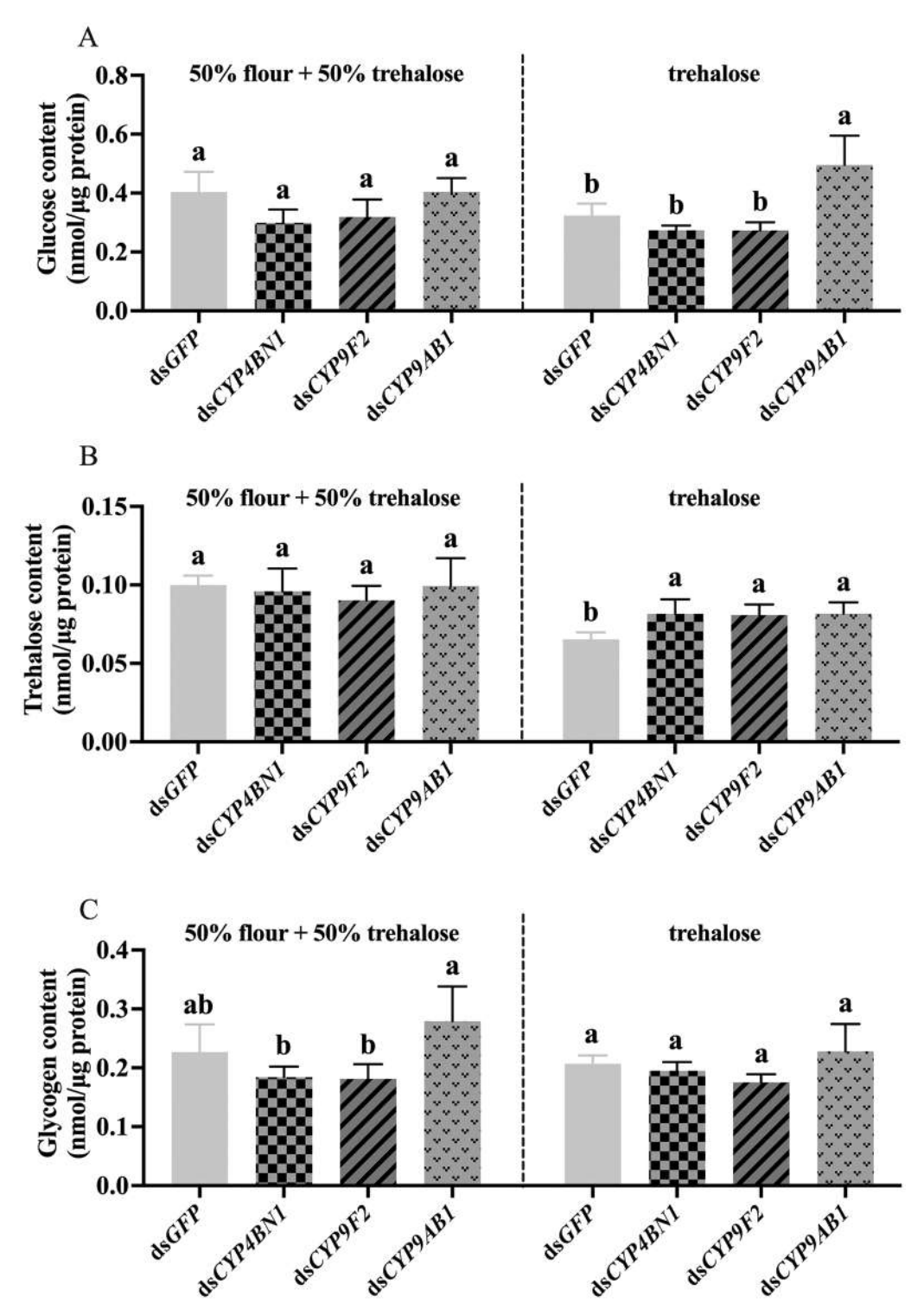


Fig. 3. The effects of trehalose dietary regimes (50% flour + 50% trehalose or 100% trehalose) and CYP gene silencing (ds *GFP*, ds *CYP94BN1*, ds *CYP9F2*, or ds *CYP9AB1*) on glucose A), trehalose B), and glycogen C) content in *T. castaneum* under 95% CO_2 stress after 48 h. Each group included 4 biological replicates with 15 larvae each. Values are presented as mean \pm SE. Different letters indicate significant differences between groups (Tukey HSD post-hoc test at α = 0.05).

Effect on CYP450 Activity under 95% CO₂ after Trehalose Feeding and dsRNA

Following a 48-h exposure to trehalose dietary regimes (50% flour + 50% trehalose or 100% trehalose) and ds CYP treatments under 95% CO₂ conditions, the CYP450 activity was assessed. On 50% flour +

50% trehalose diet, the dsCYP9AB1 group had notably higher CYP450 activity than the control, while the other 2 groups showed a slight increase (F=12.345, df=3, 12, P<0.001). On 100% trehalose diet, the CYP450 activity showed little difference among the 4 groups (F=0.772, df=3, 12, P=0.532; Fig. 5).

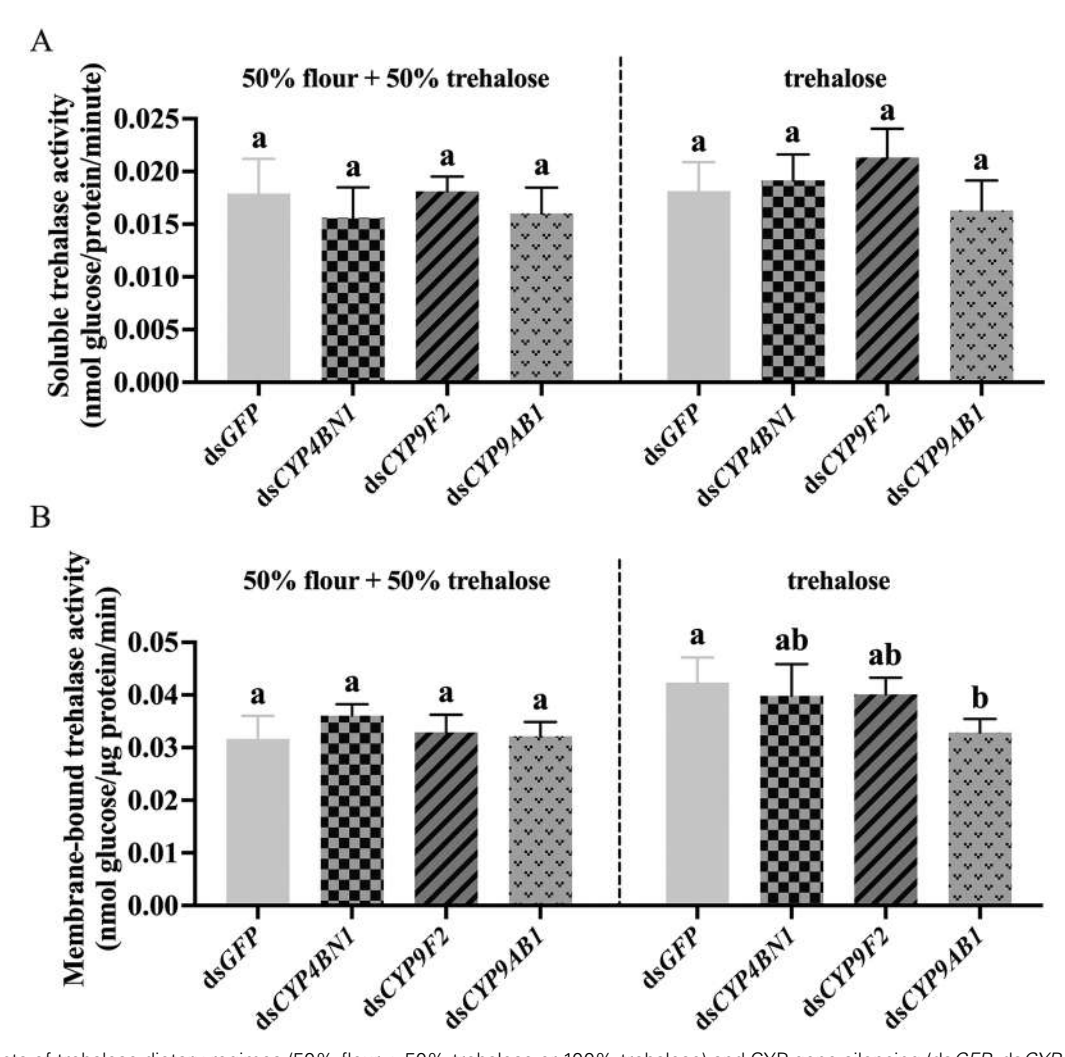
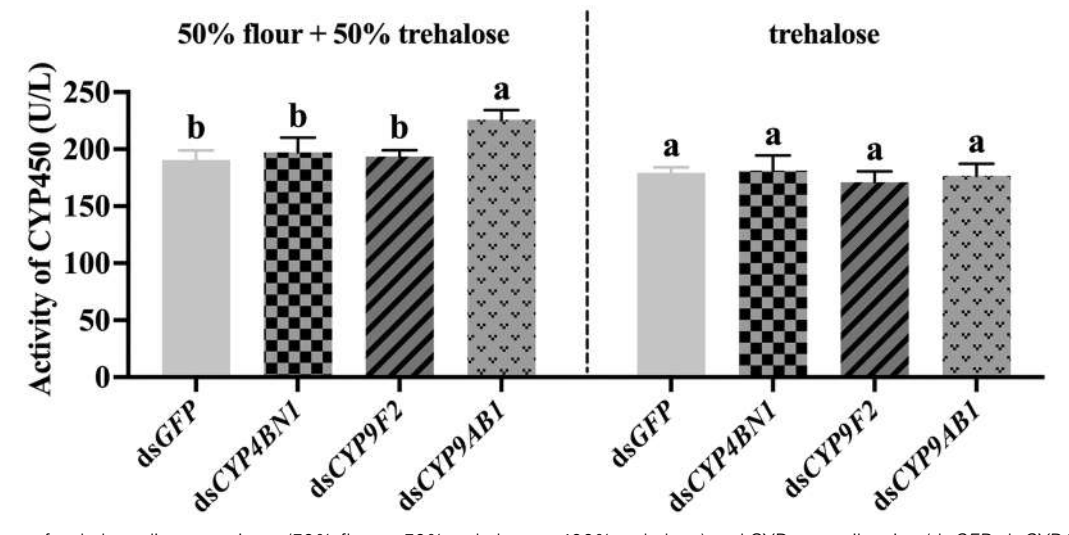


Fig. 4. The effects of trehalose dietary regimes (50% flour + 50% trehalose or 100% trehalose) and CYP gene silencing (ds GFP, ds CYP4BN1, ds CYP9F2, or ds CYP9AB1) on soluble A) and membrane-bound B) trehalase activity in T. C castaneum under 95% CO_2 stress after 48 h. Each group included 4 biological replicates with 15 larvae each. Values are presented as mean \pm SE. Different letters indicate significant differences between groups (Tukey HSD post-hoc test at α =0.05).



Effect on Trehalose Metabolism Pathway under 95% CO₂ after Trehalose Feeding and dsRNA

To investigate dsCYP impact on trehalose metabolism under 95% CO₂ and trehalose dietary regimes (50% flour + 50% trehalose or 100% trehalose), key gene expressions in the trehalose metabolic pathway were assessed. On 50% flour + 50% trehalose diet, the dsCYP4BN1 treatment significantly down-regulated TcTRE1-1, TcTRE2, TcTPS1, and TcTPS2 (TcTRE1-1: t=7.085, df=4, P=0.002; TcTRE2: t=5.168,df=4, P=0.007; TcTPS1: t=3.878, df=4, P=0.018; TcTPS2: t=4.270, df=4, P=0.013; Fig. 6A), while dsCYP9F2 decreased TcTRE1-1, TcTRE1-3, and TcTPS1 (TcTRE1-1: t=11.609, *df*=4, *P*<0.001; *TcTRE1-3*: *t*=2.810, *df*=4, *P*=0.048; *TcTPS1*: t=4.003, df=4, P=0.016; Fig. 6B). In contrast, dsCYP9AB1 up-regulated TcTRE2, TcTRE1-2, TcTRE1-3, and TcTPS2 (TcTRE2: t = -4.533, df = 4, P = 0.011: TcTRE1-2: t = -3.561,df=4, P=0.024; TcTRE1-3: t=-4.280, df=4, P=0.013; TcTPS2: t = -4.081, df = 4, P = 0.015; Fig. 6C).

On 100% trehalose diet, the dsCYP4BN1 treatment sharply reduced most genes, except for TcTRE1-3 (TcTRE1-1: t=4.013, df=4, P=0.016; TcTRE1-2: t=5.018, df=4, P = 0.007; TcTRE1-3: t = 1.548, df = 4, P = 0.196; TcTRE1-4: t=6.760, df=4, P=0.002; TcTRE2: t=4.753, df=4, P=0.009; TcTPS1: t = 4.159, df = 4, P = 0.014; TcTPS2: t = 12.827, df = 4,P<0.001; Fig. 7A). dsCYP9F2 notably increased TcTRE1-2 and decreased TcTRE1-4, with minor changes in other genes (TcTRE1-1: t=0.689, df=4, P=0.529; TcTRE1-2: t=-3.637,df=4, P=0.022; TcTRE1-3: t=-2.220, df=4, P=0.091; TcTRE1-4: t=3.990, df=4, P=0.016; TcTRE2: t=-0.175, df=4, P=0.869; TcTPS1: t=-0.822, df=4, P=0.457; TcTPS2: t = -2.696, df = 4, P = 0.054; Fig. 7B). In the dsCYP9AB1 treatment, key genes TcTRE2, TcTPS1, and TcTPS2 saw significant increases, with TcTPS2 experiencing the most pronounced upregulation (TcTRE1-1: t=-0.638, df=4, P=0.558; TcTRE1-2: t=-0.998, df=4, P=0.375; TcTRE1-3: t=-0.182, df=4, P = 0.865; TcTRE1-4: t = -1.822, df = 4, P = 0.143; TcTRE2: t=-2.869, df=4, P=0.046; TcTPS1: t=-4.402, df=4, P = 0.012; TcTPS2: t = -5.211, df = 4, P = 0.006; Fig. 7C).

Discussion

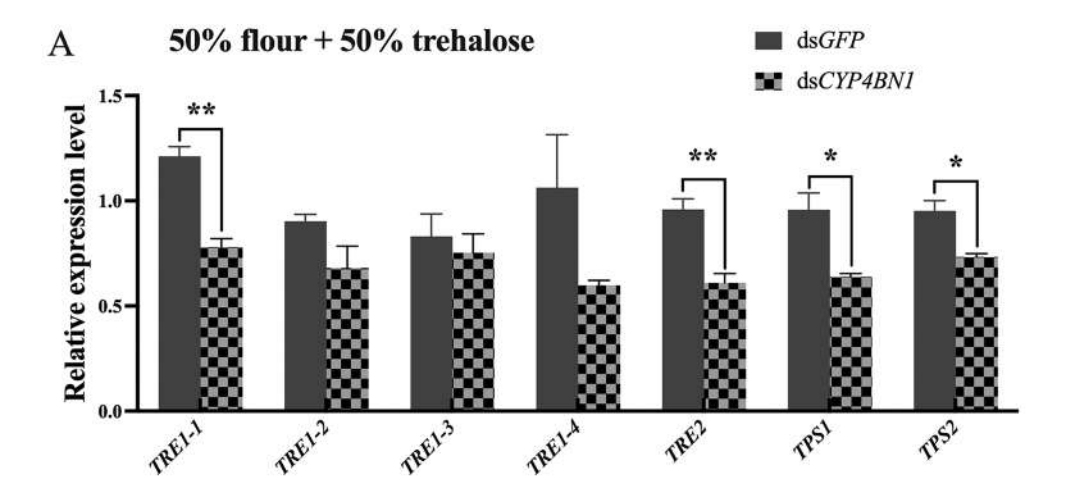
Cytochrome P450 monooxygenases are a class of important detoxification enzymes, crucial for the physiological functions of insects, while trehalose serves as a blood sugar regulator and a versatile compound that protects cells against various stress factors (Elbein et al. 2003, Kuczyńska-Wiśnik et al. 2024, Wang et al. 2024). In this study, we used qRT-PCR to analyse the expressions of *TcCYP4BN1*, *TcCYP9F2*, and *TcCYP9AB1* genes in individuals after dsRNA injection and trehalose feeding. It was found that dsRNA still maintained its inhibitory efficacy despite the presence of exogenous trehalose, as evidenced by the downregulation of CYP gene expressions (Fig. 1).

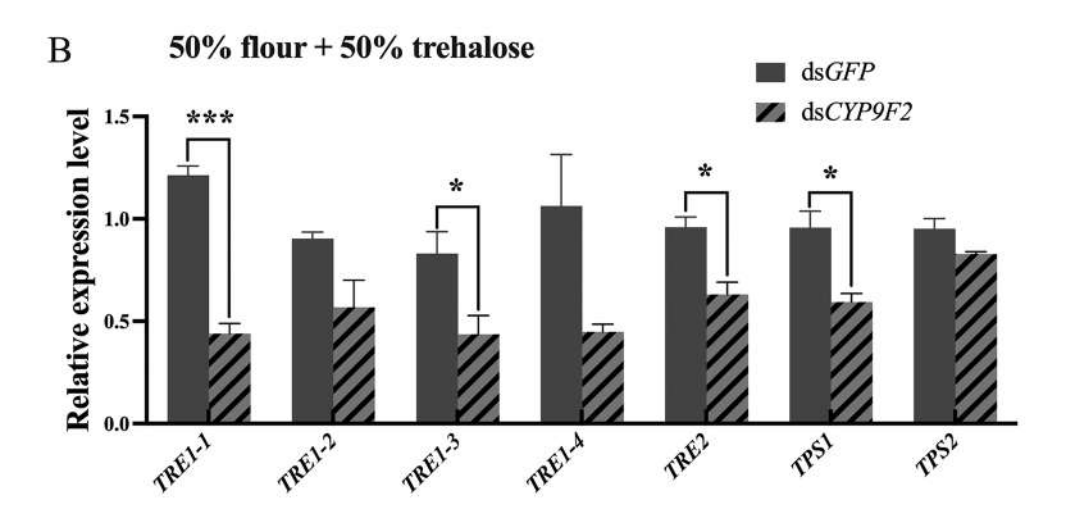
To delve deeper into the interplay between trehalose supplementation and CYP450 in *T. castaneum* under 95% CO₂, we calculated the mortality of dsCYP4BN1-, dsCYP9F2-, and dsCYP9AB1-treated groups. The results revealed that on 100% trehalose diet, dsCYP treatments still increased mortality of *T. castaneum* larvae compared with those on a mixed diet. However, under dsCYP9AB1 treatment the mortality increased on a mixed diet, but decreased surprisingly on 100% trehalose diet compared with the controls (Fig. 2). Distinct from dsCYP9AB1, dsCYP4BN1 and dsCYP9F2 treatments showed lower

mortality on a mixed diet and higher mortality on 100% trehalose diet, which was more similar to that of dsGFP (Fig. 2). This divergence suggests that TcCYP9AB1 may play a unique role in trehalose metabolism during high-CO, stress. The elevated mortality in dsCYP9AB1-treated larvae on a mixed diet implies that TcCYP9AB1 may regulate trehalose metabolism under physiological conditions, with its silencing compromising larval adaptation to high-CO2 stress. Strikingly, the reduced mortality observed in the 100% trehalose group upon TcCY-P9AB1 knockdown may point to the role of accumulated trehalose as a protector, which is known to provide energy and protection against various stress (Tellis et al. 2023). Moreover, in recent studies, a strong association has been found between CYP genes and trehalose metabolism. For example, TcCYP314A1 has been identified as effective for trehalose metabolism and synthesis of insect 20E in T. castaneum (Zhou et al. 2022). Also, when TcCYP6K1 was knocked down via RNAi, both an increased larval mortality and trehalose levels were observed in T. castaneum under 75% CO, stress (Guan et al. 2024), further emphasizing the correlation between CYP genes and trehalose metabolism. Thereby, a critical role for TcCYP9AB1 in trehalose metabolism, with a tighter link relative to the other 2 target genes, is the most likely model to account for our results.

Previously empirical evidence implies in several species, including Acyrthosiphon pisum (Harris) (Hemiptera: Aphididae) and Drosophila melanogaster (Diptera: Drosophilidae), that carbohydrate levels generally shift when insects are fed diets with varying sugar amounts as a metabolic regulatory mechanism to maintain energy homeostasis (Wang et al. 2021, Strilbytska et al. 2022). However, we observed no extremely significant biochemical changes, neither in the levels of glucose and glycogen nor in the activity of trehalase and CYP450, when T. castaneum was treated with trehalose feeding and RNAi (Figs 3–5). A potential explanation may be that stored product insects can regulate their physiological metabolic processes through their well-developed regulatory mechanisms to cope with environmental stress (Harrison et al. 2006). In Callosobruchus chinensis (Hope) (Coleoptera: Bruchidae), the magnitude of metabolic alteration under hypoxic stress showed significant fluctuations relative to controls (Cui et al. 2019), further suggesting that insects may maintain homeostasis through self-regulatory mechanisms to adapt to environmental stress. Upon closer analysis of the results, we posit that the *TcCYP9AB1* gene exhibits a stronger association with trehalose metabolism compared with the other 2 target genes, as evidenced by the significant increase in glucose content on 100% trehalose diet in the dsCYP9AB1 group, whereas the other 2 treatment groups showed decreases (Fig. 3A). Similar trends were also observed in glycogen content (Fig. 3C).

Studies have elucidated the contributions of carbohydrate metabolism to biological processes, and its critical role as a link between protein, lipid, nucleic acid, and secondary biomass metabolisms (Pan et al. 2020). Moreover, the potential regulatory mechanism underlying insect resistance to high CO₂ stress, when studied, can be fostered to facilitate the growth of sustainable storage-pest management solutions (Guan et al. 2024). Therefore, we measured the expression levels of *TcCYP4BN1*, *TcCYP9F2*, *TcCYP9AB1*, and genes related to the trehalose metabolic pathway via qRT-PCR, to further explore the intricate relationship between trehalose and CYP genes under stress conditions. Experiments evaluating the expression of related





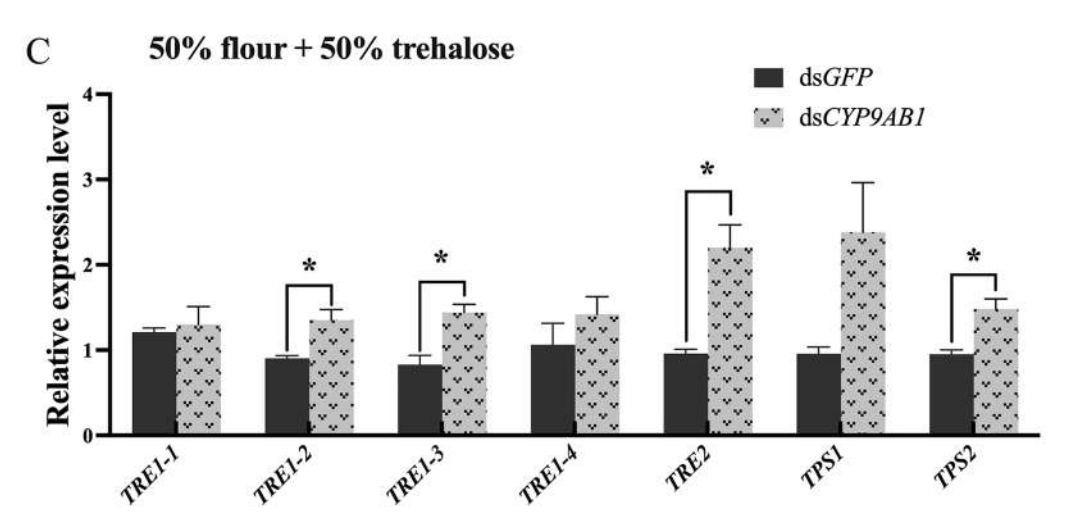
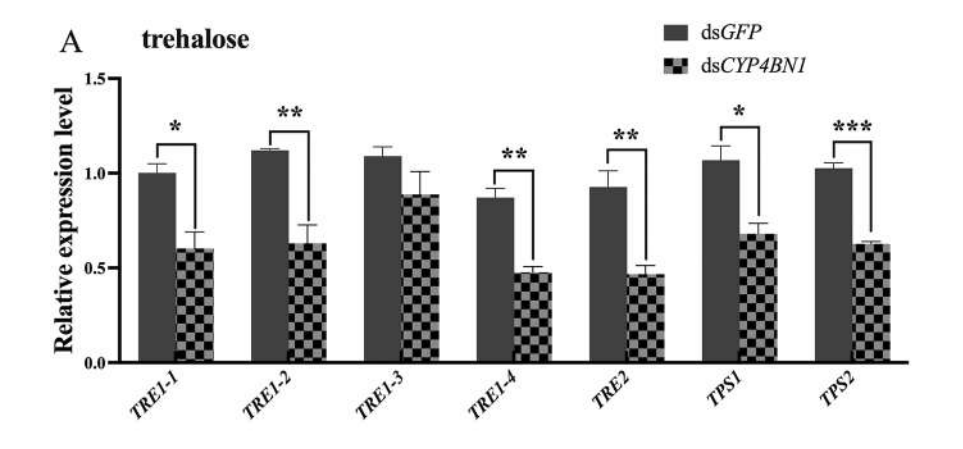
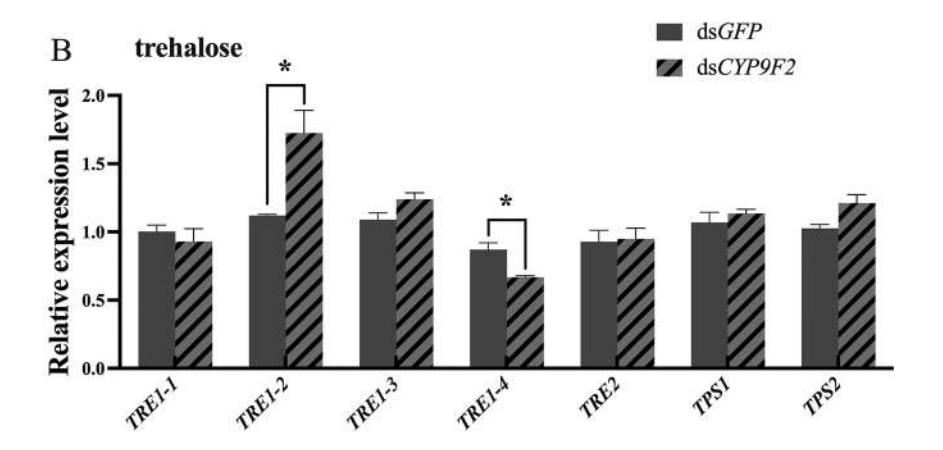


Fig. 6. On 50% flour + 50% trehalose diet, effects of ds CYP treatments on trehalose metabolic gene expression in T. castaneum under 95% CO $_2$ stress. A to C) display the impact of TcCYP4BN1 A), TcCYP9F2 B), and TcCYP9AB1 C) RNA interference on the expression of trehalose metabolic pathway genes (TRE1-1, TRE1-2, TRE1-3, TRE1-4, TRE2, TPS1, and TPS2) in larvae. TRE, trehalase; TPS, trehalose-6-posphate synthase. Each group included 3 biological replicates with 10 larvae each. Each biological replicate included 3 technical replicates. Values are presented as mean \pm SE. ***P<0.001, *P<0.01, *P<0.05 (independent samples t-test).





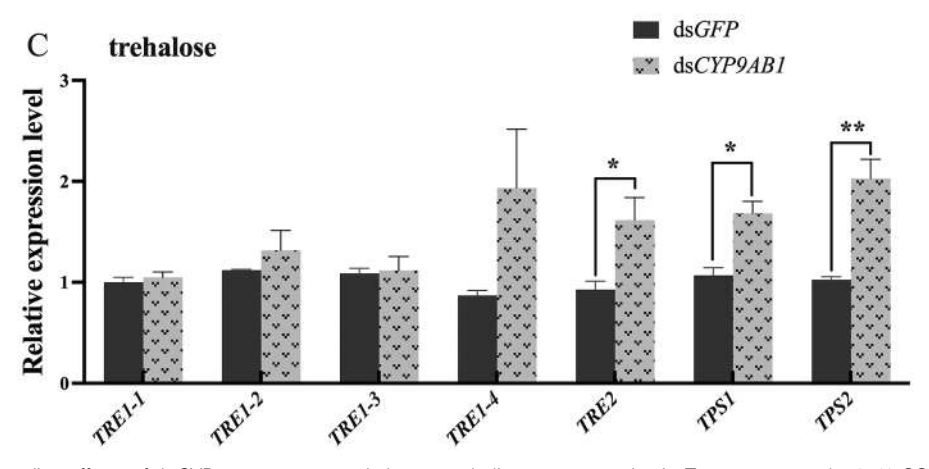


Fig. 7. On 100% trehalose diet, effects of ds*CYP* treatments on trehalose metabolic gene expression in *T. castaneum* under 95% CO₂ stress. A to C) display the impact of *TcCYP4BN1* A), *TcCYP9F2* B), and *TcCYP9AB1* C) RNA interference on the expression of trehalose metabolic pathway genes (*TRE1-1*, *TRE1-2*, *TRE1-3*, *TRE1-4*, *TRE2*, *TPS1*, and *TPS2*) in larvae. TRE, trehalose; TPS, trehalose-6-posphate synthase. Each group included 3 biological replicates with 10 larvae each. Each biological replicate included 3 technical replicates. Values are presented as mean ± SE. ***P<0.001, **P<0.01, *P<0.05 (independent samples *t*-test).

genes in all groups allowed us to confirm the possibilities that trehalose can enhance the response of CYP genes to CO₂ atmosphere stress, and that trehalose intake may alleviate the upregulation of key genes involved in trehalose metabolism caused by dsRNA, as evidenced by a decrease in the expression of genes associated with trehalose metabolism pathway in groups

exclusively fed trehalose, with the exception of the dsCYP9F2, compared with groups fed 50% flour + 50% trehalose (Figs 6 and 7). Consistent with our conjectures, trehalose and TcCYP9E2 have a synergistic effect in T. castaneum coping with high CO_2 stress (Zhou et al. 2023). Also, trehalose and TcCYP6K1 can improve the ability of T. castaneum to

withstand high CO₂ stress (Guan et al. 2024). Ultimately, our results further characterized the 3 CYP genes (*TcCYP4BN1*, *TcCYP9F2*, and *TcCYP9AB1*) which respond to high CO₂ stress and regulate trehalose metabolism in *T. castaneum*, facilitating stress resistance through trehalose accumulation.

In summary, by using RNAi to silence TcCYP4BN1, TcCYP9F2, and TcCYP9AB1 genes, our findings highlight the biological relevance of trehalose in enabling T. castaneum to withstand high CO, stress via enhancing the function of CYP genes, and reveal clear evidence of the close connection between TcCYP9AB1 and trehalose metabolism. Our study paves novel paths for delving into how T. castaneum adapts to high CO. stress, affording a panoramic view of the extensive prospects and existing boundaries of adaptive mechanisms within a dynamically transforming world. This knowledge is not only essential for understanding insects' resilience, but also has practical implications for grain storage protection. However, the specific mechanism of trehalose in coping with CO₂ stress still requires further physiological and biochemical research for clarification. Future research could delve into the molecular basis of these regulatory mechanisms, helping develop more precise biocontrol strategies and providing new solutions for pest management.

Author Contributions

Yuhang Xie (Formal analysis [equal], Investigation [equal], Methodology [equal], Writing—original draft [lead], Writing—review & editing [lead]), Min Zhou (Formal analysis [equal], Investigation [equal], Methodology [equal], Writing—original draft [equal], Writing—review & editing [equal]), Liwen Guan (Formal analysis [equal]), Writing—review & editing [equal]), Sijing Wan (Formal analysis [equal]), Writing—review & editing [equal]), Yi Zhang (Data curation [equal], Investigation [equal]), Xinyi Zhang (Data curation [equal], Investigation [equal]), Yuya Zhang (Investigation [equal], Wisualization [equal]), Yan Li (Data curation [equal]), Yan Li (Data curation [equal]), Visualization [equal]), and Bin Tang (Conceptualization [Supporting], Project administration [lead], Supervision [lead], Writing—review & editing [equal])

Funding

None declared.

Conflicts of Interest

All authors declare that they have no known competing financial interests or personal relationships that could have appeared to influence the work reported in this paper.

Data Availability

The data that support the findings of this study are available from the corresponding author upon reasonable request.

References

- Agbangba CE, Aide ES, Honfo H, et al. 2024. On the use of post-hoc tests in environmental and biological sciences: a critical review. *Heliyon* 10:e25131. https://doi.org/10.1016/j.heliyon.2024.e25131
- Badre NH, Martin ME, Cooper RL. 2005. The physiological and behavioral effects of carbon dioxide on *Drosophila melanogaster* larvae.

Comp. Biochem. Physiol. A Mol. Integr. Physiol. 140:363–376. https://doi.org/10.1016/j.cbpb.2005.01.019

- Baldwin SR, Mohapatra P, Nagalla M, et al. 2021. Identification and characterization of CYPs induced in the *Drosophila* antenna by exposure to a plant odorant. *Sci. Rep.* 11:20530. https://doi.org/10.1038/s41598-021-99910-9
- Bao J, Wang X, Feng C, et al. 2021. Trehalose metabolism in the Chinese mitten crab *Eriocheir sinensis*: molecular cloning of *trehalase* and its expression during temperature stress. *Aquac. Rep.* 20:100770. https://doi.org/10.1016/j.aqrep.2021.100770
- Chakraborty P, Biswas A, Dey S, et al. 2023. Cytochrome P450 gene families: role in plant secondary metabolites production and plant defense. *J. Xenobiot.* 13:402–423. https://doi.org/10.3390/jox13030026
- Chen Q, Behar KL, Xu T, et al. 2003. Expression of *Drosophila* trehalose-phosphate synthase in HEK-293 cells increases hypoxia tolerance. *J. Biol. Chem.* 278:49113–49118. https://doi.org/10.1074/jbc.M308652200
- Chen H, Chen C, Yu Z, et al. 2022. Comparative analyses of six cytochrome P450 genes and their roles in differential insecticide susceptibilities between the red flour beetle and the confused flour beetle. J. Stored Prod. Res. 96:101951. https://doi.org/10.1016/j.jspr.2022.101951
- Cui SF, Wang L, Qiu JP, et al. 2019. Effects of hypoxia/hypercapnia on the metablism of *Callosobruchus chinensis* (L.) larvae. *J. Stored Prod. Res.* 83:322–330. https://doi.org/10.1016/j.jspr.2019.06.002
- Cui K, Zhou L, Jiang C, et al. 2023. Residue behavior and efficacy of benzothiazole in grains under different fumigation conditions. *Pest Manag. Sci.* 79:3622–3630. https://doi.org/10.1002/ps.7536
- Delacre M, Lakens D, Mora Y, et al. 2018. Taking parametric assumptions seriously arguments for the use of Welch's F-test instead of the classical F-test in One-way ANOVA (in press for the International Review of Social Psychology). https://doi.org/10.31234/osf.jo/wnezg
- Elbein AD, Pan YT, Pastuszak I, et al. 2003. New insights on trehalose: a multifunctional molecule. *Glycobiology* 13:17R–27R. https://doi.org/10.1093/glycob/cwg047
- Ge X, Shi Y, Wang S, et al. 2021. Sequence analysis of *Harmonia axyridis* pyruvate kinase gene and its regulation of trehalose metabolism. *Sci. Agric. Sin.* 54:5021–5031.
- Guan L, Wang X, Wan S, et al. 2024. The role of *TcCYP6K1* and *TcCYP9F2* influences trehalose metabolism under high-CO₂ Stress in *Tribolium castaneum* (Coleoptera). *Insects* 15:502. https://doi.org/10.3390/insects15070502
- Harrison J, Frazier MR, Henry JR, et al. 2006. Responses of terrestrial insects to hypoxia or hyperoxia. *Respir. Physiol. Neurobiol.* 154:4–17. https://doi.org/10.1016/j.resp.2006.02.008
- Huang L, Ruan L, Guo Y, et al. 2024a. The effect of trehalose on the contents of starch and oil in microalga *Dunaliella parva*. Algal Res. 81:103600. https://doi.org/10.1016/j.algal.2024.103600
- Huang Y, Wang D, Jian F, et al. 2024b. Plodia interpunctella larvae exposed to 2% O₂ with or without 4% CO₂ showed changes in chemical substances, enzyme activities, body mass, and water content. J. Stored Prod. Res. 108:102358. https://doi.org/10.1016/j.jspr.2024.102358
- Ingegno BL, Tavella L. 2022. Ozone gas treatment against three main pests of stored products by combination of different application parameters. J. Stored Prod. Res. 95:101902. https://doi.org/10.1016/j. jspr.2021.101902
- Kaur A, Singh S, Sharma SC. 2024. Unlocking Trehalose's versatility: a comprehensive Journey from biosynthesis to therapeutic applications. *Exp. Cell Res.* 442:114250. https://doi.org/10.1016/j.yexcr.2024. 114250
- Kim K, Gao H, Li C, et al. 2024. The glutathione biosynthesis is involved in metamorphosis, antioxidant function, and insecticide resistance in *Tribolium castaneum. Pest Manag. Sci.* 80:2698–2709. https://doi. org/10.1002/ps.7976
- Kuczyńska-Wiśnik D, Stojowska-Swędrzyńska K, Laskowska E. 2024. Intracellular protective functions and therapeutical potential of trehalose. *Molecules* 29:2088. https://doi.org/10.3390/molecules 29092088

- Livak KJ, Schmittgen TD. 2001. Analysis of relative gene expression data using real-time quantitative PCR and the 2-ΔΔCT method. *Methods* 25:402–408. https://doi.org/10.1006/meth.2001.1262
- Long G-Y, Yang X-B, Wang Z, et al. 2024. Wing expansion functional analysis of ion transport peptide gene in Sogatella furcifera (Horváth) (Hemiptera: Delphacidae). Comp. Biochem. Physiol. B Biochem. Mol. Biol. 271:110946. https://doi.org/10.1016/j.cbpb.2024.110946
- Manandhar A, Milindi P, Shah A. 2018. An overview of the post-harvest grain storage practices of smallholder farmers in developing countries. *Agriculture* 8:57. https://doi.org/10.3390/agriculture8040057
- Natonek-Wiśniewska M, Krzyścin P, Koseniuk A. 2022. Qualitative and quantitative detection of mealworm DNA in raw and commercial food products using real-time PCR. *Genes. (Basel)* 13:1400. https:// doi.org/10.3390/genes13081400
- National Center for Biotechnology Information. 2024a. *Tribolium castaneum CYP4BN1*, mRNA sequence. (NCBI Nucleotide Database). Identifier: NM_001130521. https://www.ncbi.nlm.nih.gov/nuccore/NM_001130521.
- National Center for Biotechnology Information. 2024b. *Tribolium castaneum CYP9F2*, mRNA sequence. (NCBI Nucleotide Database). Identifier: NM_001134234. https://www.ncbi.nlm.nih.gov/nuccore/NM_001134234.
- National Center for Biotechnology Information. 2024c. Tribolium castaneum CYP9AB1, mRNA sequence. (NCBI Nucleotide Database). Identifier: XM_967453. https://www.ncbi.nlm.nih.gov/nuccore/XM_967453.
- Osanai M, Kojima KK, Futahashi R, et al. 2006. Identification and characterization of the telomerase reverse transcriptase of *Bombyx mori* (silkworm) and *Tribolium castaneum* (flour beetle). *Gene* 376:281–289. https://doi.org/10.1016/j.gene.2006.04.022
- Pan B, Xu K, Luo Y, et al. 2020. The sequence characteristics and functions on regulating trehalose metabolism of two PTP genes in *Tribolium castaneum* (Herbst) (Coleoptera: Tenebrionidae). *J. Stored Prod. Res.* 89:101692. https://doi.org/10.1016/j.jspr.2020.101692
- Paul A, Radhakrishnan M, Anandakumar S, et al. 2020. Disinfestation techniques for major cereals: a status report. Compr. Rev. Food Sci. Food Saf. 19:1125–1155. https://doi.org/10.1111/1541-4337.12555
- Pender CL, Horvitz HR. 2018. Hypoxia-inducible factor cell non-autonomously regulates *C. elegans* stress responses and behavior via a nuclear receptor. Kaeberlein M, Stainier DY, editors. *eLife* 7:e36828. https://doi.org/10.7554/eLife.36828
- Ribeiro GD, de Holanda Paranhos L, Eleutherio ECA. 2024. Trehalose promotes biological fitness of fungi. *Fungal Biol.* 128:2381–2389. https://doi.org/10.1016/j.funbio.2024.03.004
- Sadeghi R, Heidari F, Ebadollahi A, et al. 2021. High-pressure carbon dioxide use to control dried apricot pests, *Tribolium castaneum* and *Rhyzopertha Dominica*, and assessing the qualitative traits of dried pieces of treated apricot. *Foods* 10:1190. https://doi.org/10.3390/ foods10061190
- Sang W, Ma W-H, Qiu L, et al. 2012. The involvement of heat shock protein and cytochrome P450 genes in response to UV-A exposure in the beetle *Tribolium castaneum*. *J. Insect Physiol*. 58:830–836. https://doi.org/10.1016/j.jinsphys.2012.03.007
- Shelomi M. 2022. Cytochrome P450 genes expressed in phasmatodea midguts. *Insects* 13:873. https://doi.org/10.3390/insects13100873
- Singh V, Louis J, Ayre BG, et al. 2011. TREHALOSE PHOSPHATE SYNTHASE11 - dependent trehalose metabolism promotes Arabidopsis thaliana defense against the phloem - feeding insect Myzus persicae. Plant J. 67:94–104. https://doi.org/10.1111/j.1365-313X. 2011.04583.x
- Strilbytska O, Semaniuk U, Bubalo V, et al. 2022. Dietary choice reshapes metabolism in *Drosophila* by affecting consumption of macronutrients. *Biomolecules* 12:1201. https://doi.org/10.3390/biom12091201
- Tan S, Li G, Guo H, et al. 2023. RNAi-mediated silencing of AccCYP6k1 revealed its role in the metabolic detoxification of Apis cerana cerana. Pestic. Biochem. Physiol. 191:105377. https://doi.org/10.1016/j.pestbp.2023.105377

- Tang B, Wei P, Zhao L, et al. 2016. Knockdown of five trehalase genes using RNA interference regulates the gene expression of the chitin biosynthesis pathway in *Tribolium castaneum*. BMC Biotechnol. 16:67. https://doi.org/10.1186/s12896-016-0297-2
- Tao Y-D, Liu Y, Wan X-S, et al. 2023. High and low temperatures differentially affect survival, reproduction, and gene transcription in male and female moths of *Spodoptera frugiperda*. *Insects* 14:958. https://doi.org/10.3390/insects14120958
- Tellis MB, Kotkar HM, Joshi RS. 2023. Regulation of trehalose metabolism in insects: from genes to the metabolite window. *Glycobiology* 33:262–273. https://doi.org/10.1093/glycob/cwad011
- Wang K, Liu M, Wang Y, et al. 2020. Identification and functional analysis of cytochrome P450 CYP346 family genes associated with phosphine resistance in *Tribolium castaneum*. *Pestic. Biochem*. *Physiol*. 168:104622. https://doi.org/10.1016/j.pestbp.2020. 104622
- Wang T, Liu X, Luo Z, et al. 2024. Transcriptome-wide identification of cytochrome P450s in tea black tussock moth (*Dasychira baibarana*) and candidate genes involved in Type-II sex pheromone biosynthesis. *Insects* 15:139. https://doi.org/10.3390/insects15020139
- Wang W, Yu H, Kim HS, et al. 2019. Molecular characterization of a sweet potato stress tolerance-associated trehalose-6-phosphate synthase 1 gene (*IbTPS1*) in response to abiotic stress. *Plant Biotechnol. Rep.* 13:235–243. https://doi.org/10.1007/s11816-019-00532-5
- Wang G, Zhou J-J, Li Y, et al. 2021. Trehalose and glucose levels regulate feeding behavior of the phloem-feeding insect, the pea aphid *Acyrthosiphon pisum* Harris. *Sci. Rep.* 11:15864. https://doi.org/10.1038/s41598-021-95390-z
- Watanabe M. 2006. Anhydrobiosis in invertebrates. *Appl. Entomol. Zool.* 41:15–31. https://doi.org/10.1303/aez.2006.15
- Wu Z-Q, Guan L-W, Pan B-Y, et al. 2022. Mechanism of *HIF1*-α-mediated regulation of *Tribolium castaneum* metabolism under high CO₂ concentration elucidated. *J. Stored Prod. Res.* 99:102030. https://doi.org/10.1016/j.jspr.2022.102030
- Xu K-K, Pan B-Y, Wang Y-Y, et al. 2020. Roles of the *PTP61F* gene in regulating energy metabolism of *Tribolium castaneum* (Coleoptera: Tenebrionidae). *Front. Physiol.* 11:1071. https://doi.org/10.3389/fphys.2020.01071
- Yao J, Chen C, Wu H, et al. 2019. Differential susceptibilities of two closely-related stored product pests, the red flour beetle (*Tribolium* castaneum) and the confused flour beetle (*Tribolium confusum*), to five selected insecticides. J. Stored Prod. Res. 84:101524. https://doi. org/10.1016/j.jspr.2019.101524
- Yu W, Pan B, Qiu L, et al. 2020. The structure characteristics and biological functions on regulating trehalose metabolism of two NITret1s in Nilaparvata lugens. Sci. Agric. Sin 53:4802–4812. 2020.
- Zhang Y, Gao S, Xue S, et al. 2021. Disruption of the cytochrome P450 CYP6BQ7 gene reduces tolerance to plant toxicants in the red flour beetle, *Tribolium castaneum*. *Int. J. Biol. Macromol.* 172:263–269. https://doi.org/10.1016/j.ijbiomac.2021.01.054
- Zhang N, Jiang H, Meng X, et al. 2020. Broad-complex transcription factor mediates opposing hormonal regulation of two phylogenetically distant arginine kinase genes in *Tribolium castaneum*. *Commun. Biol.* 3:631. https://doi.org/10.1038/s42003-020-01354-w
- Zhang H, Li H, Fang S, et al. 2024. Co-application of Validamycin A and dsRNAs targeting *trehalase* genes conferred enhanced insecticidal activity against *Laodelphax striatellus*. *Pestic. Biochem. Physiol*. 205:106160. https://doi.org/10.1016/j.pestbp.2024.106160
- Zhang L, Qiu L-Y, Yang H-L, et al. 2017. Study on the effect of wing bud chitin metabolism and its developmental network genes in the brown Planthopper, *Nilaparvata lugens*, by knockdown of *TRE* gene. *Front. Physiol.* 8:750. https://doi.org/10.3389/fphys. 2017.00750
- Zhang L, Zhao H, Yang Y, et al. 2022. Effects of nutritional composition of different prey eggs on development and reproduction of the predatory bug, *Orius sauteri* (Hemiptera: Anthocoridae). *J. Econ. Entomol.* 115:1869–1876. https://doi.org/10.1093/jee/toac159

Zhou Z-X, Dou W, Li C-R, et al. 2022. CYP314A1-dependent 20-hydroxyecdysone biosynthesis is involved in regulating the development of pupal diapause and energy metabolism in the Chinese citrus fruit fly, *Bactrocera minax*. *Pest Manag. Sci.* 78:3384–3393. https://doi.org/10.1002/ps.6966

- Zhou Y-F, Zhou M, Wang Y-Y, et al. 2023. Characterization of the *TcCYPE2* gene and its role in regulating trehalose metabolism in response to high CO₂ stress. *Agronomy* 13:2263. https://doi.org/10.3390/agronomy13092263
- Zhu M, Zhang W, Liu F, et al. 2016. Characterization of an *Apis cerana* cerana cytochrome P450 gene (*AccCYP336A1*) and its roles in oxidative stresses responses. *Gene* 584:120–128. https://doi.org/10.1016/j.gene.2016.02.016
- Zou X, Wang S, Cheng Q, et al. 2024. N-terminal truncated trehalose-6-phosphate synthase 1 gene (△NIbTPS1) enhances the tolerance of sweet potato to abiotic stress. *Plant Physiol. Biochem.* 214:108917. https://doi.org/10.1016/j.plaphy.2024.108917